Nuclear Instruments and Methods in Physics Research A ∎ (∎∎∎∎) ∎∎∎–∎∎∎

Contents lists available at ScienceDirect

Nuclear Instruments and Methods in Physics Research A

journal homepage: www.elsevier.com/locate/nima

Study of surface properties of ATLAS12 strip sensors and their radiation resistance

M. Mikestikova [s,*], P.P. Allport [a], M. Baca [a], J. Broughton [a], A. Chisholm [a], K. Nikolopoulos [a], S. Pyatt [a], J.P. Thomas [a], J.A. Wilson [a], J. Kierstead [b], P. Kuczewski [b], D. Lynn [b], L.B.A. Hommels [c], M. Ullan [d], I. Bloch [e], I.M. Gregor [e], K. Tackmann [e], M. Hauser [f], K. Jakobs [f], S. Kuehn [f], K. Mahboubi [f], R. Mori [f], U. Parzefall [f], A. Clark [g], D. Ferrere [g], S. Gonzalez Sevilla [g], J. Ashby [h], A. Blue [h], R. Bates [h], C. Buttar [h], F. Doherty [h], T. McMullen [h], F. McEwan [h], V. O'Shea [h], S. Kamada [i], K. Yamamura [i], Y. Ikegami [j], K. Nakamura [j], Y. Takubo [j], Y. Unno [j], R. Takashima [k], A. Chilingarov [l], H. Fox [l], A.A. Affolder [m], G. Casse [m], P. Dervan [m], D. Forshaw [m,l], A. Greenall [m], S. Wonsak [m], M. Wormald [m], V. Cindro [n], G. Kramberger [n], I. Mandić [n], M. Mikuž [n], I. Gorelov [o], M. Hoeferkamp [o], P. Palni [o], S. Seidel [o], A. Taylor [o], K. Toms [o], R. Wang [o], N.P. Hessey [p], N. Valencic [p], K. Hanagaki [q,j], Z. Dolezal [r], P. Kodys [r], J. Bohm [s], J. Stastny [s], A. Bevan [t], G. Beck [t], C. Milke [u], M. Domingo [u], V. Fadeyev [u], Z. Galloway [u], D. Hibbard-Lubow [u], Z. Liang [u], H.F.-W. Sadrozinski [u], A. Seiden [u], K. To [u], R. French [v], P. Hodgson [v], H. Marin-Reyes [v], K. Parker [v], O. Jinnouchi [w], K. Hara [x,y], K. Sato [x,y], M. Hagihara [x], S. Iwabuchi [x], J. Bernabeu [z], J.V. Civera [z], C. Garcia [z], C. Lacasta [z], S. Marti i Garcia [z], D. Rodriguez [z], D. Santoyo [z], C. Solaz [z], U. Soldevila [z]

[a] School of Physics and Astronomy, University of Birmingham, Birmingham B15 2TT, United Kingdom
[b] Brookhaven National Laboratory, Physics Department and Instrumentation Division, Upton, NY 11973-5000, USA
[c] Cavendish Laboratory, University of Cambridge, JJ Thomson Avenue, Cambridge CB3 0HE, United Kingdom
[d] Centro Nacional de Microelectronica (IMB-CNM, CSIC), Campus UAB-Bellaterra, 08193 Barcelona, Spain
[e] DESY, Notkestrasse 85, 22607 Hamburg, Germany
[f] Physikalisches Institut, Universität Freiburg, Hermann-Herder-Str. 3, D-79104 Freiburg, Germany
[g] DPNC, University of Geneva, 24, Quai Ernest-Ansermet, CH-1211 Geneve 4, Switzerland
[h] SUPA – School of Physics and Astronomy, University of Glasgow, Glasgow G12 8QQ, United Kingdom
[i] Solid State Div., Hamamatsu Photonics K.K., 1126-1, Ichino-cho, Higashi-ku, Hamamatsu-shi, Shizuoka 435-8558, Japan
[j] Institute of Particle and Nuclear Study, KEK, Oho 1-1, Tsukuba, Ibaraki 305-0801, Japan
[k] Department of Science Education, Kyoto University of Education, Kyoto 612-8522, Japan
[l] Physics Department, Lancaster University, Lancaster LA1 4YB, United Kingdom
[m] Oliver Lodge Laboratory, Department of Physics, University of Liverpool, Oxford St., Liverpool L69 7ZE, United Kingdom
[n] Jožef Stefan Institute and Department of Physics, University of Ljubljana, Ljubljana, Slovenia
[o] Department of Physics and Astronomy, University of New Mexico, MSC07 4220, 1919 Lomas Blvd. NE, Albuquerque, NM 87131, USA
[p] Nikhef, Science Park 105, 1098 XG Amsterdam, The Netherlands
[q] Department of Physics, Osaka University, Machikaneyama-cho 1-1, Toyonaka-shi, Osaka 560-0043, Japan
[r] Charles University in Prague, Faculty of Mathematics and Physics, V Holesovickach 2, Prague 8, Czech Republic
[s] Academy of Sciences of the Czech Republic, Institute of Physics, Na Slovance 2, 18221 Prague 8, Czech Republic
[t] School of Physics and Astronomy, Queen Mary University of London, London E1 4NS, United Kingdom
[u] Santa Cruz Institute for Particle Physics (SCIPP), University of California, Santa Cruz, CA 95064, USA
[v] Department of Physics and Astronomy, The University of Sheffield, Hicks Building, Hounsfield Road, S3 7RH Sheffield, United Kingdom
[w] Institute of Science and Engineering, Tokyo Institute of Technology, Ookayama 2-12-1, Meguro-ku, Tokyo 152-8551, Japan
[x] Institute of Pure and Applied Sciences, University of Tsukuba, Tsukuba, Ibaraki 305-8751, Japan
[y] Center for Integrated Research in Fundamental Science and Engineering, University of Tsukuba, Tsukuba, Ibaraki 305-8571, Japan
[z] IFIC/CSIC-UVEG, Ed. Inst. Investigacion, PO Box 22085, 46071 Valencia, Spain

* Corresponding author.
E-mail address: mikestik@fzu.cz (M. Mikestikova).

http://dx.doi.org/10.1016/j.nima.2016.03.056
0168-9002/

ARTICLE INFO

Article history:
Received 20 November 2015
Received in revised form
3 March 2016
Accepted 16 March 2016

Keywords:
HL-LHC
ATLAS ITk
Micro-strip sensor
Radiation resistance
Surface properties
Inter-strip capacitance
Inter-strip resistance
Punch-through protection

ABSTRACT

A radiation hard n^+-in-p micro-strip sensor for the use in the Upgrade of the strip tracker of the ATLAS experiment at the High Luminosity Large Hadron Collider (HL-LHC) has been developed by the "ATLAS ITk Strip Sensor collaboration" and produced by Hamamatsu Photonics.

Surface properties of different types of end-cap and barrel miniature sensors of the latest sensor design ATLAS12 have been studied before and after irradiation. The tested barrel sensors vary in "punch-through protection" (PTP) structure, and the end-cap sensors, whose stereo-strips differ in fan geometry, in strip pitch and in edge strip ganging options. Sensors have been irradiated with proton fluences of up to 1×10^{16} n_{eq}/cm^2, by reactor neutron fluence of 1×10^{15} n_{eq}/cm^2 and by gamma rays from ^{60}Co up to dose of 1 MGy. The main goal of the present study is to characterize the leakage current for micro-discharge breakdown voltage estimation, the inter-strip resistance and capacitance, the bias resistance and the effectiveness of PTP structures as a function of bias voltage and fluence. It has been verified that the ATLAS12 sensors have high breakdown voltage well above the operational voltage which implies that different geometries of sensors do not influence their stability. The inter-strip isolation is a strong function of irradiation fluence, however the sensor performance is acceptable in the expected range for HL-LHC. New gated PTP structure exhibits low PTP onset voltage and sharp cut-off of effective resistance even at the highest tested radiation fluence. The inter-strip capacitance complies with the technical specification required before irradiation and no radiation-induced degradation was observed. A summary of ATLAS12 sensors tests is presented including a comparison of results from different irradiation sites. The measured characteristics are compared with the previous prototype of the sensor design, ATLAS07.

1. Introduction

The Phase-II upgrade of the Large Hadron Collider (LHC) to the higher luminosity (5×10^{34} cm^{-2} s^{-1}) machine, called the High Luminosity-LHC (HL-LHC) [1], will require replacement of the entire current ATLAS Inner Detector with a new all-silicon tracker containing new type and design of silicon sensors. It will have pixel sensors at the inner radii surrounded by micro-strips. As currently planned, the micro-strip detector in the upgraded Inner Tracker (ITk) [2,3] will consist of 2 barrel layers of "short" strips (length 23.8 mm), 2 barrel layers of "long" strips (length 47.8 mm) and seven end-cap discs on each side. The end-cap strips length varies from 15 mm to 60 mm depending on the radius. The strip length is chosen so as to maintain the average hit occupancy to be less than 1% at the expected maximum instantaneous luminosity. The maximum hit occupancy is limited by the bandwidth of the read-out system.

Strip sensors in the ITk will be exposed to charged particles, neutrons and gammas. The predicted maximum fluence and ionizing dose [4] for the integrated luminosity of 3000 fb^{-1} in the strip barrels is 5.3×10^{14} 1-MeV neutron equivalent (n_{eq})/cm^2 and 216 kGy for the short strips in the layer 1, and in the strip end-caps 8.1×10^{14} n_{eq}/cm^2 and 288 kGy in the inner regions of the outermost disk at a distance of 300 cm from interaction point. The estimates stated above have no safety factors applied. Such a high fluence of particles and ionizing dose causes bulk and surface damage to the sensors. In this study the miniature sensors were irradiated by protons, neutrons and gammas from ^{60}Co source. Protons and neutrons displace silicon atoms via non-ionizing energy losses, which results in point and cluster defects in the bulk. In addition protons ionize both the Si bulk and the insulating layer (SiO_2). The latter causes the accumulation of positive charges and traps in the SiO_2 and at the Si-SiO_2 interface that leads to deterioration of the sensor surface. The gamma irradiation is usually used to study the oxide/interface damage separately from the bulk damage. However, gamma rays from ^{60}Co source are absorbed in the sensor mainly through Compton scattering and the scattered Compton electrons have high enough energy (hundreds of keV) to produce point defects in the Si bulk. The surface damage is expected to influence the breakdown voltage, the inter-electrode isolation and capacitance.

The current ATLAS Semi-Conductor Tracker is based on single-sided type of micro-strip sensors made with p-strips implanted on n-type silicon bulk (p-in-n). n^+-in-p type sensors, which are much more radiation hard [5,6], are being considered for use in the HL-LHC trackers. This type of sensor has much faster response as it collects electrons instead of holes. It also has no radiation induced type inversion and therefore it always depletes from the segmented side that allows sensor operation in partially depleted mode. This is particularly useful after high radiation fluencies when the full depletion voltage becomes higher. However, n^+-in-p strip sensors need additional strip isolation.

A large area n^+-in-p silicon sensor for the use in ITk has been developed by the ATLAS ITk Strip Sensor Collaboration [7,8] and produced by Hamamatsu Photonics (HPK) [9] in a 6-inch (150 mm) wafer. Besides the large sensor (9.75 cm × 9.75 cm), the wafer also includes sets of miniature sensors, which are used for irradiation studies. The sensors were irradiated by different particles, energies and doses and were distributed for extensive test to many institutions of the collaboration for studies of sensor properties that have received up to double maximal fluence predicted in ITk.

The samples for the surface irradiation study presented in this paper are the barrel and end-cap (EC) miniature strip sensors of the latest sensor design, called ATLAS12 [8] which was developed from ATLAS07 design [7]. The surface properties before and after ionizing radiation up to the proton fluence of 1×10^{16} n_{eq}/cm^2, neutron fluence 1×10^{15} n_{eq}/cm^2 and gamma dose of up to 1 MGy were evaluated. The tests include measurements of the inter-strip capacitance and resistance as a function of fluence, and the inter-strip resistance as a function of bias, temperature and annealing time. The effectiveness of different types of punch-through protection structures was tested with DC voltage scan method.

Some of the surface studies with previous design ATLAS07 were reported in Ref. [10] to maximal fluence of 1.5×10^{13} n_{eq}/cm^2. The bulk damage of latest design ATLAS12 is presented in Ref. [11] for barrel and in Ref. [12] for end-cap sensors.

Please cite this article as: M. Mikestikova, et al., Nuclear Instruments & Methods in Physics Research A (2016), http://dx.doi.org/10.1016/j.nima.2016.03.056

2. Samples and irradiation

The tested sensors of ATLAS12A, ATLAS12M and ATLAS07 layouts[1] are fabricated in *p*-type, float zone wafers with $<1\,0\,0>$ crystal orientation and thickness of 320 μm. For each layout, slightly different wafer resistivity was used, and therefore the full depletion voltage (V_{FD}) differs. The V_{FD} of non-irradiated sensors, estimated from capacitance-voltage measurements of strip miniature sensors, was typically 350–360 V for 12 A, 225 V for 12 M, and 200 V for 07.

The readout aluminum strips are capacitively coupled with *n*-strips biased through polysilicon resistors. The strip isolation is done with common *p*-implant (*p*-stop) with surface ion concentration of approximately 4×10^{12} cm^{-2}. The tested sensors are $\sim1\times1$ cm^2. The barrel sensors have 74.5 μm strip pitch with various "punch-through protection" (PTP) structure geometries examined. The end-cap sensors evaluated here have stereo-strips in fan geometry that differ in strip pitch ("large" and "small" pitches: 103.4 and 64.3 μm on average, respectively) and in edge strip biasing. Details of the design including strip isolation structure and the edge strips ganging are described in Ref. [8].

The proton irradiations were performed at Karlsruhe Inst. Tech., Germany (KIT) [13] with 23 MeV, at Birmingham, UK [14] with 27 MeV and at CYRIC (Tohoku University, Japan) with 70 MeV protons. Samples were kept in a cooled box during irradiations and the box was scanned to cover the whole target area of sensors. The stage scan speed at the CYRIC irradiation was 20 mm/s, at KIT 115 mm/s and at the Birmingham 1 mm/s (2013 irradiation run) and 4 mm/s (2015 run). The scan time depends on the beam current and the area of the samples to be irradiated at the same run. The 10^{15} n_{eq}/cm^2 fluence took 15 min at KIT at a beam current 1.7 μA, ~80 s in the Birmingham cyclotron at 1000 nA (2013 run), and ~100 min at CYRIC at 400 nA (2015 run) and at 700 nA (2014 run). The measurement of the equivalent proton fluence has an error of approximately 20%, taking the precision of the dosimetry and of the estimation of hardness factor into account. The irradiated samples were immediately stored in a refrigerator to prevent any post-irradiated annealing. The neutron irradiations were achieved at Ljubljana JSI TRIGA Reactor [15]. The accuracy of neutron fluence is 10%. The source of uncertainty is the precision of the dosimetry and errors in timing of irradiation. ^{60}Co gamma irradiation was carried out at the Solid State Gamma-ray irradiation facility of the Brookhaven National Laboratory (BNL) [16] and at the Institute of Nuclear Fuels, Prague (UJP) [17]. The sensors were maintained at room temperature during gamma irradiation. The dose rate was 220 Gy/hour and 13.2 kGy/hour in BNL and UJP, respectively. The dose rate uncertainty is ~10% in both cases.

3. Punch-through protection structures

AC coupled strip sensors can be subjected to large voltages between the readout metal strips and the implant strips. These large voltages can be caused by charge accumulation in the bulk due to beam splash accidents. A dedicated punch-through protection (PTP) structure, at the ends of the implant strips is used to keep the implant voltage low. The PTP structure creates a short-circuit in current path in parallel to the bias resistor at the voltages higher than the PTP onset voltage, thus avoiding the capacitor breakdown. The ATLAS12 miniature sensors have different types of PTP structures (A–F type) (Fig. 1) [8]. The E and F types are standard PTP structure with 20 and 70 μm gap between the bias ring and the end of the implant n^+-strip. The B and C types are new, improved PTP structure with an extended polysilicon electrode of the bias ring over the PTP gap; so called the full-gate structures.

4. Experimental methods and results

About 200 miniature sensors of different types have been tested for surface studies before and after irradiations at silicon laboratories at the Academy of Sciences of the Czech Republic in Prague, University of California Santa Cruz, University of Tsukuba, University of Freiburg, Lancaster University and IFIC Valencia. The sensors were either bonded to PCB board and measured in temperature control box down to −50 °C or in probe station with a cooled chuck where the contact was provided by micro-manipulators (down to −30 °C). Nitrogen environment ensured humidity below 5% at 20 °C.

4.1. Leakage current

The leakage current as a function of the bias voltage (IV) was measured for all types of the barrel and end-cap sensors in order to determine whether sensor stability is influenced or not by sensor geometry, wafer used and surface radiation damage. For all the tested non-irradiated sensors, the value of the leakage current at 600 V is less than 4.8 nA/cm^2 at 20 °C, which is well below the technical specification's limit (<2 μA/cm^2) [18]. There were no observed onsets of micro-discharges in any of the sensors up to 1000 V.

The upper plot of Fig. 2 shows the current of the proton irradiated ATLAS12A, 12 M and 07 barrel sensors. The lower plot of Fig. 2 shows the current of the end-cap sensors irradiated by protons and gammas. Neutron irradiated barrel sensor is included for comparison. All sensors were measured after annealing them for 80 min at 60 °C. Most of the proton irradiated sensors did not show micro-discharge breakdown below 1000 V. The wiggle at 250–350 V in low fluence samples (0.52 and 1×10^{13} n_{eq}/cm^2) is probably due to surface generated current in the backside electrode – when the depletion had reached the backside [8]. The average current values at bias voltage 600 V and temperature −10 °C are 30, 51 and 103 μA/cm^2 for the proton fluence 0.5, 1 and 2×10^{15} n_{eq}/cm^2, respectively. The leakage current increase with fluence is consistent with bulk current increase. The values correspond to what one would expect from the estimate $I(\Phi,t,T)=\alpha(t,T)V\Phi$, where α is the leakage current damage factor,[2] V is the active sensor volume and Φ is fluence in n_{eq}/cm^2. Measured current value above fluence of 1×10^{15} n_{eq}/cm^2 is lower than what is estimated using the sensor volume because sensors are not fully depleted at 600 V. The full depletion voltage increases with increasing proton fluence except for a little variation at low fluence – the V_{FD} decreases up to 1×10^{14} n_{eq}/cm^2 due to initial acceptor removal process [21]. The V_{FD} of ATLAS12 sensors is 350–450 V and 500–700 V for 3×10^{14} and 1×10^{15} n_{eq}/cm^2, respectively. At fluences greater than 3×10^{15} n_{eq}/cm^2 the V_{FD} is above 1000 V.

The total leakage current increases ~100 times after gamma irradiation, which is the result of the surface current increase due to surface damage. Unfortunately, the guard ring in the tested sensors does not have a probing pad and thus it is not possible to separate the leakage current of the active area inside of the bias ring from the current at the periphery. The micro-discharge breakdown at 900 V of sensors irradiated by 10 kGy gamma dose

[1] In ATLAS12A wafer layout the large-area main sensor is made of all "axial" strips where the strips are parallel to the sensor edge. In ATLAS12M two segments of strips are "axial" and two are "stereo" strips where the strips are inclined to the sensor edge. More details about 12 A and 12 M wafer design are in [8].

[2] $\alpha=4\times10^{-17}$ A/cm^2 at 20 °C after annealing for $t=80$ min at 60 °C [19]. Bulk current temperature normalization with activation energy of 1.2 eV was used.

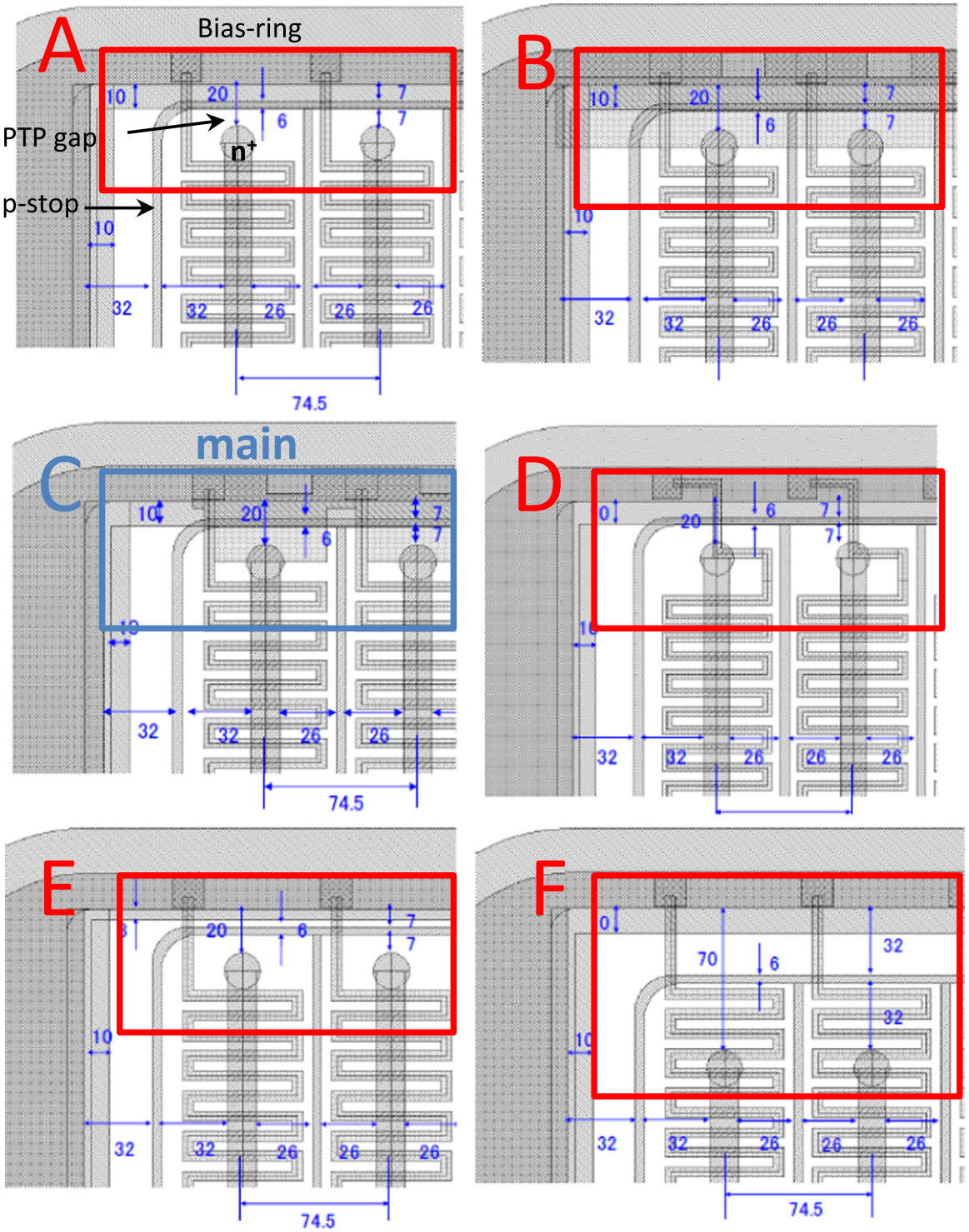

Fig. 1. PTP structures in ATLAS12 miniature sensors. New PTP structure with full gate (C-type) is implemented in main ATLAS12 sensor in addition to the miniature test sensors.

is attributed to surface damage [22]. It is well above the maximum operating voltage 600 V and it disappears after annealing and additional irradiation. Observation that the current is lower for the higher gamma dose is a subject of further studies.

4.2. Inter-strip capacitance

Important strip sensor surface characteristics which give us information about the effect of surface radiation damage are the inter-strip capacitance (C_{int}) and inter-strip resistance (R_{int}). The inter-strip capacitance contributes to the input capacitance of the readout electronics and is the main contributor to the detector noise. Therefore, it should be as low as possible. The capacitance is measured by LCR meter between a central metal strip and its nearest neighbors with other strips floating (Fig. 3). This way the measurement also includes additional ~10% contribution from the next neighbors [23,10].

The inter-strip capacitance before irradiation was measured on 25 ATLAS12 sensors at 100 kHz test frequency as required by specifications. The average values of C_{int} are equal to 0.76 ± 0.02,

Please cite this article as: M. Mikestikova, et al., Nuclear Instruments & Methods in Physics Research A (2016), http://dx.doi.org/10.1016/j.nima.2016.03.056

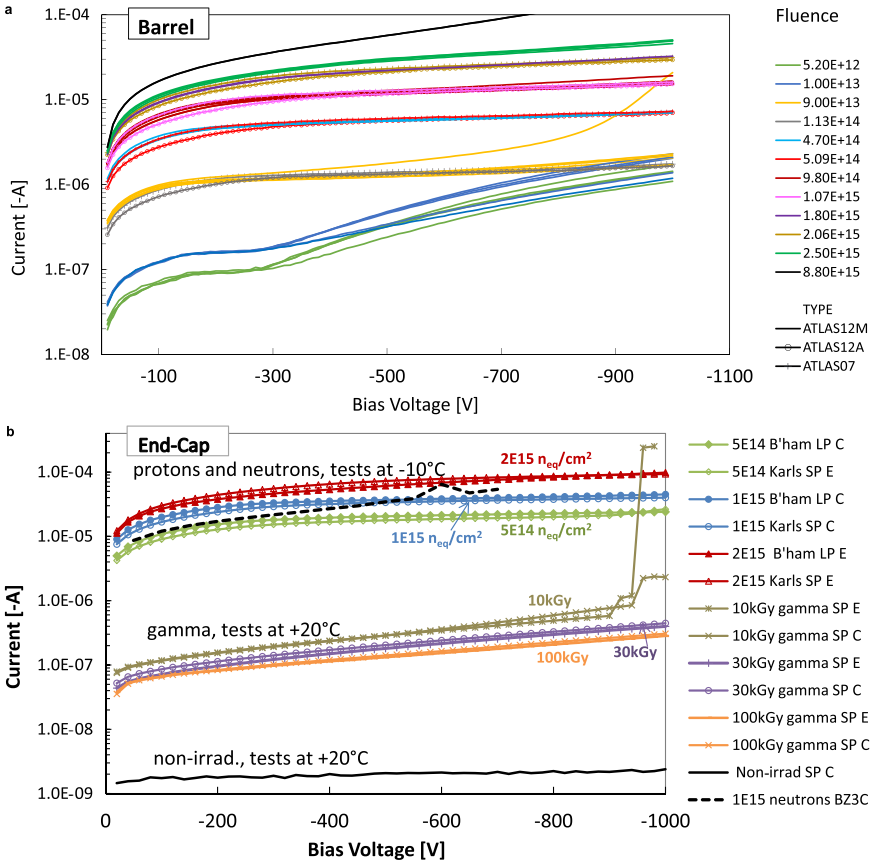

Fig. 2. The leakage current vs. bias voltage after annealing 80 min at 60 °C for (upper) ATLAS12A, 12 M and 07 barrel sensors irradiated by protons (CYRIC) to fluences in range 0.52×10^{13}–8.8×10^{15} n_{eq}/cm^2 taken at −20 °C and for (lower) various types of ATLAS12 end-cap sensors after proton (Birmingham and Karlsruhe), gamma and neutron irradiation compared with non-irradiated sensor. Proton and neutron sensors were measured at −10 °C, gamma and non-irradiated ones at room temperature +20 °C [20]. SP and LP in the legend denote for small and large pitch sensors, respectively; E and C are referring to different PTP structure types.

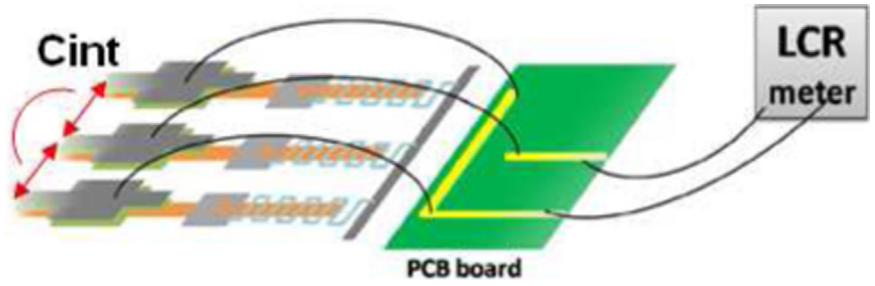

Fig. 3. Measuring method for the inter-strip capacitance: AC pads of metal strips are bonded to PCB board. The capacitance between the central strip and its neighbors is measured by an LCR meter in parallel mode.

0.79 ± 0.01 and 0.55 ± 0.01 pF/cm for barrel, small and large pitch end cap sensors, respectively. The value for the barrel miniature sensors is in very good agreement with value of large area sensor having the same strip pitch [24]. The bias voltage dependence of C_{int} was measured at different proton fluences and gamma doses at test frequency 1 MHz.[3] Fig. 4a shows the results for gamma irradiation. The higher the radiation dose the higher the value of the bias voltage needed for C_{int} to saturate to the pre-radiation value. This is caused by the surface effect when the increasing charge trapped in the oxide upon irradiation induces an increase in carrier concentration in thin accumulation layer between strips. Beyond V_{FD} the C_{int} becomes constant for both types of irradiation and for all tested doses. C_{int} is not influenced by the PTP structure type. In the case of gamma irradiation, the V_{FD} does not change with irradiation dose, unlike of the proton irradiation. At high proton fluences the depletion depth does not reach the full thickness of the sensor and small increase in values of measured C_{int} at 400 V is probably due to the contribution of the strip-to-backplane capacitance (C_{bulk}) as seen in Fig. 4b. Fig. 5 shows the C_{int} as a function of proton fluence of ATLAS12A, 12 M and 07 measured at various institutions. The inter-strip capacitance is wafer independent and does not change with proton fluence at high bias.

4.3. Inter-strip resistance

A well performing strip sensor has to have a good isolation between the strips in order to maintain the high spatial resolution

[3] The inter-strip capacitance measurements are dependent on the frequency of the AC signal. There is a radiation induced resonance at 10 kHz that increases with increasing proton fluence and also affects measurements of C_{int} at 100 kHz [20]. Therefore, for irradiated sensors the higher test frequency of 1 MHz was used. The resonance effect is not present at this value.

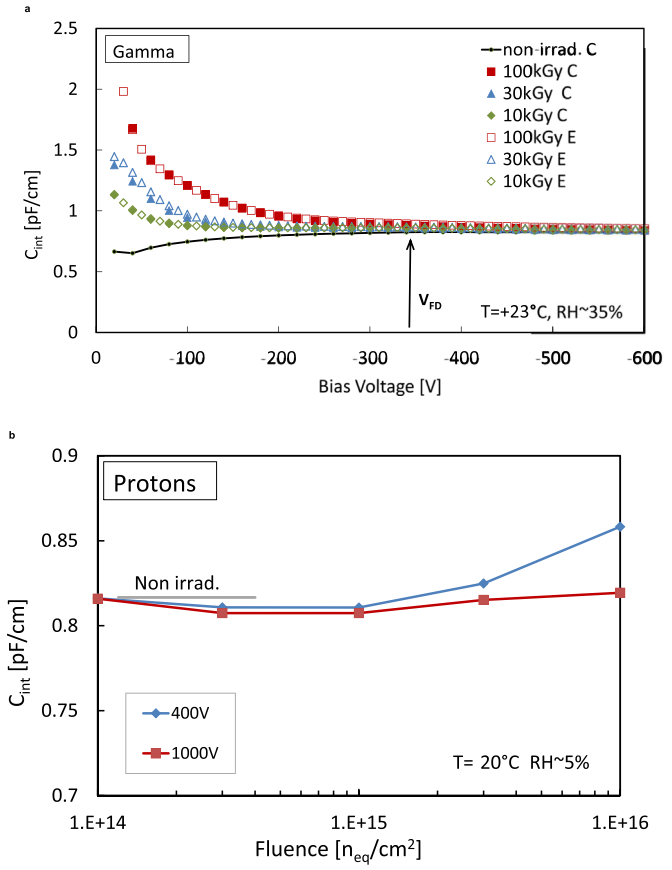

Fig. 4. (a) Inter-strip capacitance as a function of bias voltage: ATLAS12A end-cap sensors of small pitch (C and E PTP type) irradiated by gamma. Unirradiated sensor value shown for comparison. Beyond V_{FD} the C_{int} saturates to pre-radiation value. (b) Inter-strip capacitance vs. proton fluence measured at bias voltage −400 V and −1000 V: ATLAS12A barrel sensors. The measurements were done at 1 MHz.

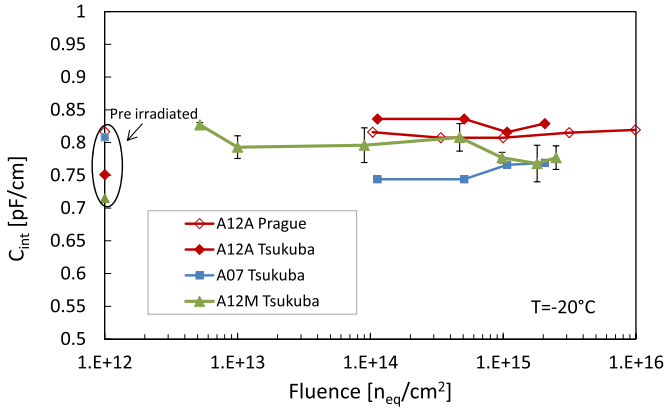

Fig. 5. Proton fluence dependence of inter-strip capacitance. ATLAS12A, 12 M and 07 barrel sensors. V_{bias} = −1000 V.

and adequate signal level of the recorded hits. The isolation between neighboring strips was verified by measurements of the inter-strip resistance (R_{int}). The measuring method is illustrated on Fig. 6. Three adjacent DC pads were contacted. Voltage V_{app} was applied by the Source-Measurement Unit to the central strip and the current I_{int} was measured on the outer strips. The measurements were performed at +20 °C for non-irradiated sensors and at cold temperatures (from −10 °C to −50 °C) for irradiated ones. The inter-strip resistance was calculated by

$$R_{int} = 2 / (dI_{int} / dV_{app}).$$

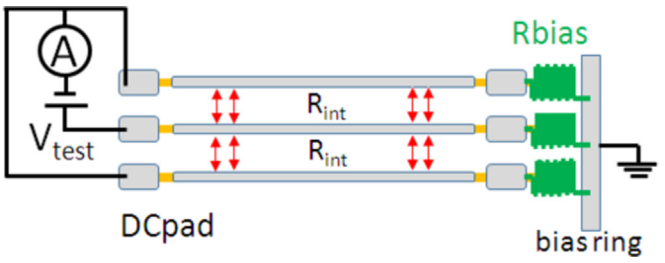

Fig. 6. Measurement set-up for inter-strip resistance measurement. The applied voltage was in range (−5V, +5 V) for non-irradiated sensors with low inter-strip currents (~100's pA) and (−1 V,+1 V) for irradiated sensors. Bias voltage was applied to the sensor up to −1000 V.

The inter-strip resistance values of non irradiated sensors are tens of GΩ's which significantly exceeds the minimum limit $10 \times R_{bias} \sim 15$ MΩ required in the technical specification [18]. The inter-strip resistance as a function of bias voltage for ATLAS12A sensors irradiated by protons at different fluences from 1×10^{14} to 1×10^{16} n_{eq}/cm^2 is shown in Fig. 7. A non-irradiated sample is also shown for comparison. The sensors with PTP structure of type C and E are compared. Before irradiation the inter-strip resistance is independent of bias voltage. After proton irradiation the inter-strip resistance is reduced and is bias voltage dependent. The bias field decreases conductivity between strips. The results of various institutions are consistent. No dependence on PTP structure type was observed.

The inter-strip current as a function of applied voltage for sensors irradiated to different proton fluences is shown in Fig. 8a. The inter-strip current is linear function of applied voltage up to the highest proton fluence 1×10^{16} n_{eq}/cm^2. The total leakage current is in this case 124 μA. The Fig. 8b presents a comparison of proton and neutron irradiated sensors with the same fluence of 1×10^{15} n_{eq}/cm^2. Both sensors have a high total leakage current of 26 μA (at $V_{bias} = -300$V), but the neutron irradiated sensor has a high $R_{int} = 5.28 \pm 0.14$ GΩ, whereas proton irradiated sensor has lower $R_{int} = 0.92 \pm 0.01$ GΩ.

The inter-strip resistance of irradiated sensors is temperature dependent as illustrated in Fig. 9. The inter-strip current has the same temperature dependence as bulk generation current. Using the activation energy of 1.2 eV, the values of inter-strip resistance, normalized to −20 °C, are very consistent in the range −10 °C to −25 °C at which sensors were measured in various laboratories (right plot of Fig. 9). In a larger range from 0 °C to −50°C the inter-strip resistance values are also very close.

The ATLAS12A, 12 M and 07 barrel sensors were irradiated in the same irradiation campaign for comparison. Inter-strip resistance as a function of proton fluence measured at various laboratories at the bias voltage 400 V is shown in Fig. 10. All sensor types have the same inter-strip resistance degradation with proton fluence. Inter-strip resistance values exceed the minimum specs limit up to 3×10^{15} n_{eq}/cm^2. Up to 1×10^{16} n_{eq}/cm^2 the inter-strip resistance is still larger than the pre-amplifier input impedance of < 1 kΩ for the ABC130 chip [25].

The correlations between the total ionizing dose (TID) and inter-strip resistance has been studied by comparison of proton, neutron and gamma irradiated sensors. Due to the different damage mechanism caused by proton and gamma in silicon sensor, the proton fluence was converted to TID by:

$$TID = \frac{\Phi[n_{eq}/cm^2]}{\kappa}\left(\frac{dE}{dx}\right)_{E_p},$$

where Φ is the proton fluence given by irradiation facilities in 1 MeV neutron equivalent, $\left(\frac{dE}{dx}\right)_{E_p}$ is the stopping power of protons of energy E_p in silicon taken from tables in [26] and κ is the

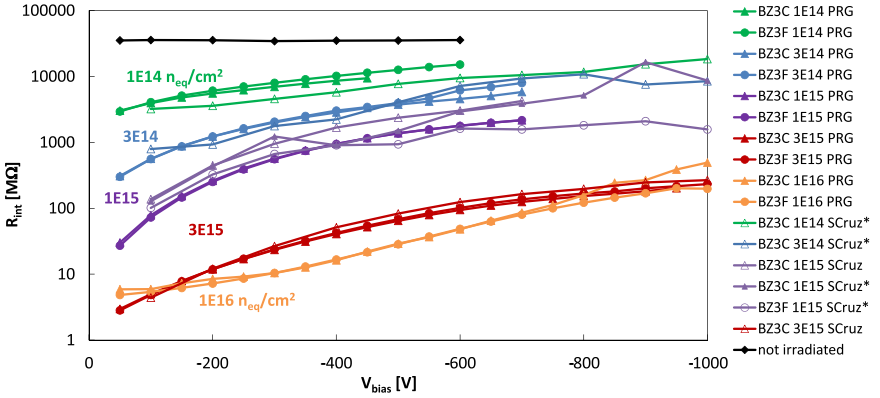

Fig. 7. The inter-strip resistance as a function of bias voltage for non- irradiated and proton irradiated (CYRIC) sensors ATLAS12A. The inter-strip resistance values are normalized to −20 °C. C and F in the legend denote for PTP structure type, (*) for not annealed sensors.

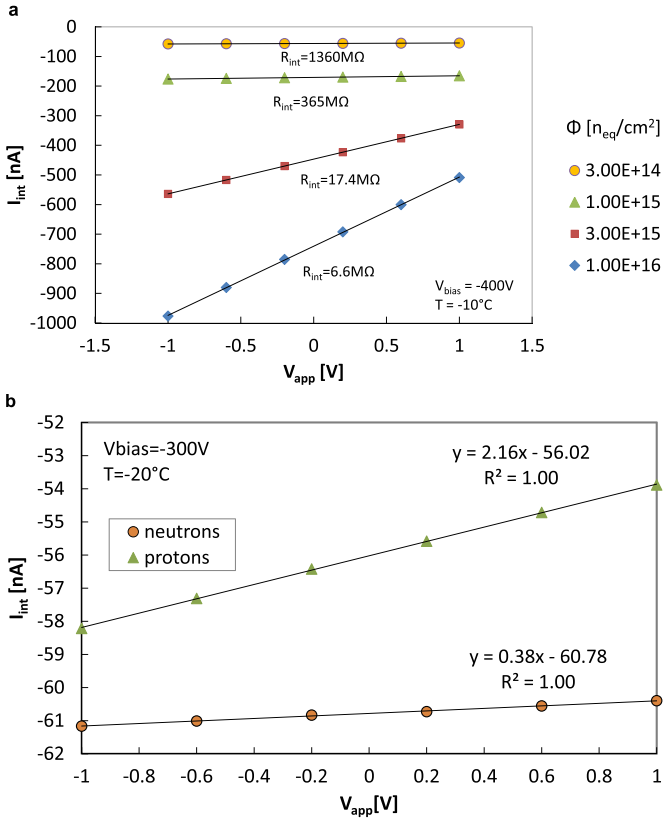

Fig. 8. The inter-strip current as a function of applied voltage: (a) comparison of different proton fluences and (b) comparison of proton and neutron irradiated sensors to the same fluence of 1×10^{15} n_{eq}/cm^2. The inter-strip current is linear function of applied voltage.

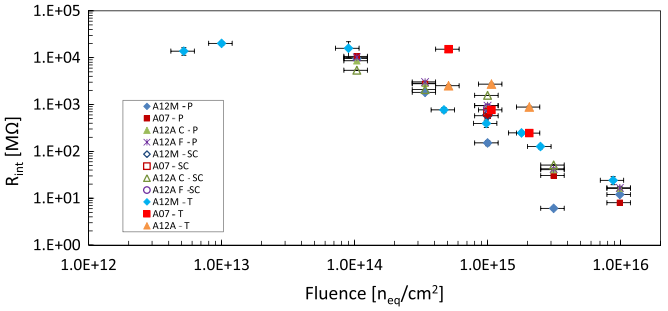

Fig. 10. Inter-strip resistance vs. proton fluence for ATLAS12A, 12 M and 07 barrel samples irradiated in the same irradiation campaign at CYRIC and measured by various laboratories at bias voltage of −400 V. The results are normalized to temperature of −20 °C.

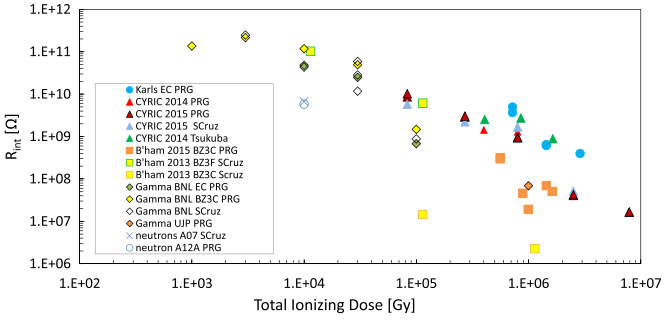

Fig. 11. Inter-strip resistance vs. total ionizing dose for ATLAS12 sensors irradiated by protons, neutrons and gammas at different irradiation sites. Results at bias voltage −400 V are presented. The values are normalized to the temperature of −20 °C.

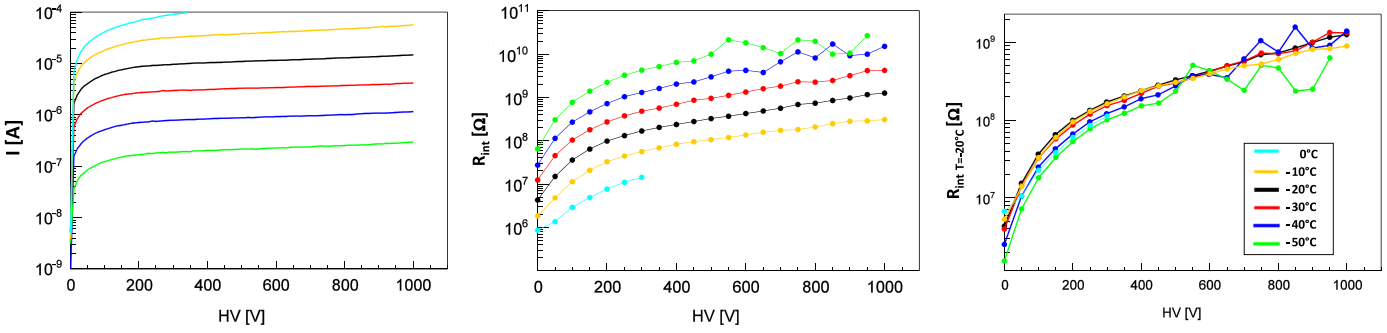

Fig. 9. Temperature dependence of total leakage current (left) and inter-strip resistance (middle) measured in temperature interval from −50 °C to 0 °C. Inter-strip resistance is normalized to −20 °C using E_a=1.2 eV (right). The measured sample is ATLAS12M barrel sensor irradiated to fluence of 1×10^{15} n_{eq}/cm^2.

conversion damage factor (κ is 1.5, 2.2 and 2 for CYRIC, Birmingham and Karlsruhe irradiation, respectively [27]). In proton irradiated samples the fluence of 1×10^{15} n_{eq}/cm^2 then corresponds to 0.80, 1.13 and 1.44 MGy for CYRIC, Birmingham and Karlsruhe irradiation, respectively. The TID in neutron irradiated sensors due to secondary particles has been assessed to be 10 kGy for 1×10^{15} n_{eq}/cm^2 [28]. The dependence of inter-strip resistance on TID is presented in Fig. 11. Gamma and proton irradiated sensors have a similar dependence of inter-strip resistance on the TID, underscoring the influence of the surface damage on the strip isolation. Exceptions are samples from Birmingham 2013 irradiation campaign. This discrepancy is a subject of further studies and tests at the Birmingham facility.

We further sought to check the influence of the bulk damage on the strip isolation by studying neutron irradiated sensors. They have one order of magnitude lower inter-strip resistance than gamma irradiated ones at the same TID. Neutrons in silicon, unlike gammas, cause mainly bulk damage resulting in increased leakage current. The leakage current of gamma irradiated sensors is more than 100 times lower than in neutron ones. Assuming that the TID dose determination for the neutron samples is sufficiently accurate, the difference indicates that the inter-strip resistance may be affected by the bulk damage by its current dependence in addition to the lead effect of the surface damage by TID.

To study the annealing effect on inter-strip resistance, a proton irradiated sensor (2×10^{15} n_{eq}/cm^2) was submitted to successive annealing steps at 60 °C up to total time of 44,000 min. The results of this study are presented in Fig. 12. The annealing of the leakage current is shown for comparison. The leakage current shows typical annealing behavior – decrease at low bias voltage with annealing time and increase at high voltage as charge multiplication (CM) appears at longer annealing. With annealing time the space charge concentration rises and higher electric field near strips causes CM [29]. Inter-strip resistance shows opposite behavior related to leakage current – significant increase at low bias voltage with annealing time and decrease at higher voltage. Annealing for 5000 min causes inter-strip resistance increase to pre-rad value, but the leakage current is still 4 orders of magnitude higher than before irradiation. Charge multiplication near the strips influences the inter-strip resistance at 700 V after annealing for 5000 min and at 400 V at more than 22,000 min.

4.4. Coupling capacitance and bias resistance

The coupling capacitance (C_{coupl}) was measured between strip metal and strip implant at 1 kHz test frequency. The values of C_{coupl}/cm achieved are greater than 24 pF for both non-irradiated and proton irradiated sensors, which meets the specifications of C_{coupl}/cm >20 pF [18].

The direct method was used for an estimate of the bias resistance. A current–voltage scan was performed applying voltages (V_{app}) from -1 to $+1$ V in 0.4-V steps to the implant DC pad, and measuring the implant strip current (I_{impl}). I_{impl} is a linear function of applied voltage and resistivity (R_{bias}) was estimated as $R_{bias}=dV_{app}/dI_{impl}$. Gamma and proton irradiated sensors have much lower inter-strip resistance, and inter-strip currents influence the bias resistance measurements. To eliminate these inter-strip effects the voltage V_{test} was applied also on two neighbors, and on next neighbors at the same time. IV was performed on the central strip.

The polysilicon bias resistance of non-irradiated sensors is 1.48 ± 0.07 MΩ which is well within the specification's range ($R_{bias}=1.5 \pm 0.5$ MΩ). It slightly increases with proton fluence and gamma dose. However it agrees with the specification up to proton fluence of 3×10^{15} n_{eq}/cm^2 and gamma dose 1 MGy.

4.5. Stability measurements

Possible time evolution of leakage current and surface parameters is an important operational aspect for strip sensor. Therefore the stability of the leakage current, as well as the inter-strip capacitance and resistance was studied by applying the bias voltage to the sensors for a few hours. Measurements performed at low temperature (from -10 °C to -25 °C) and low humidity verified that the inter-strip capacitance and resistance does not change in time. The leakage current showed relatively small decrease up to 3% during 20 h in some sensors. The results are in agreement with previous studies for the current Semiconductor tracker of ATLAS experiment [30].

4.6. Punch-through protection

The effectiveness of the punch-through protection structure was tested by using the static DC method [10,31,32]. The test voltage V_{test} (0–100 V) was applied between the implant (DC pad) and the grounded bias rail and resulting current I_{test} was recorded. The I_{test} consists of the punch-through current I_{PTP} and the current flowing through the polysilicon bias resistor (the bias resistance $R_{bias} \approx 1.5$ MΩ). The punch-through onset voltage $V_{PTP\ onset}$ is then defined to be the test voltage at which $I_{PTP}=10$ μA. A well functioning PTP structure demands low $V_{PTP\ onset}$, a steep current I_{PTP} increase above $V_{PTP\ onset}$ along with maximal current flow below

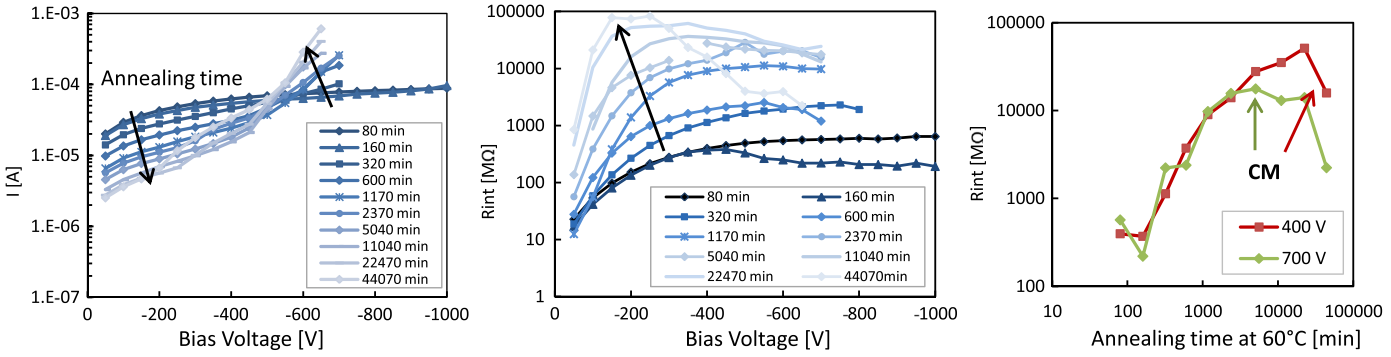

Fig. 12. The leakage current (left) and the inter-strip resistance (middle) measured at different annealing time at 60 °C, inter-strip resistance vs. annealing time (right) measured at 400 V and 700 V. ATLAS12A sensor irradiated by proton fluence 2×10^{15} n_{eq}/cm^2 (Karlsruhe) was studied. The arrows in the left and middle plot indicate the data trends with the annealing time.

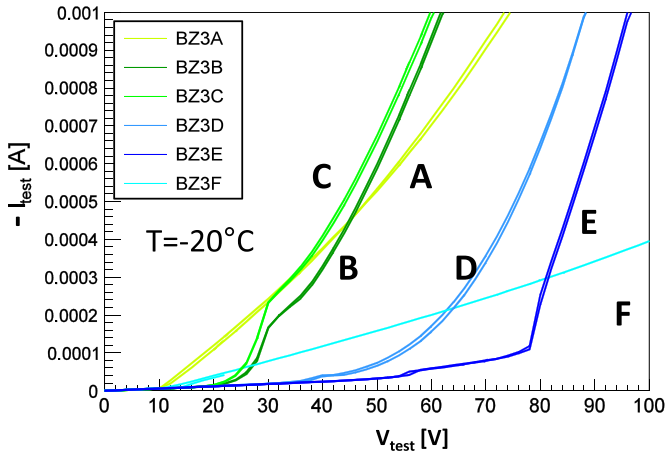

Fig. 13. Current I_{test} as a function of applied test voltage V_{test} for different types of PTP structures (A–F) implemented in ATLAS12M sensors. Sensors were irradiated by protons to fluence of 1×10^{15} $n_{eq}/cm^2$and measured at bias voltage 1000 V and temperature −20 °C.

100 V. The measured current I_{test} as a function of the test voltage for various PTP structure types for proton irradiated sensors at 1×10^{15} n_{eq}/cm^2 is shown in Fig. 13 while the PTP onset voltage and current at 100 V are shown in Fig. 14.

The full gate structures C and B exhibit the steepest increase in current while keeping $V_{PTP\ onset}$ low. In addition the C type have the modest increase of PTP onset voltage up to 2×10^{15} n_{eq}/cm^2 and large current I_{PTP} ($@V_{PTP}$= 100 V)=2.5 mA even at 1×10^{16} n_{eq}/cm^2 (Figs.13 and 14). The novel full gate PTP structure C doubles the allowable current without increasing the onset voltage.

5. Summary and conclusions

Surface properties of ATLAS12 n^+-in-p strip sensors intended for upgraded ATLAS ITk fabricated by Hamamatsu were evaluated by several participating institutes to verify if they can cope with predicted high radiation environment. Different types of barrel and end-cap miniature sensors were tested. Sensors have high micro-discharge breakdown before and after irradiation which is well above the maximum operational voltage (500–600 V). The results show that sensor stability is not influenced by PTP structure type, strip pitch, type of edge strip ganging or the wafer used. The inter-strip capacitance of all types of sensors is less than 0.9 pF/cm which complies with specifications and does not change with irradiation. The inter-strip resistance decreases with proton, neutron and gamma irradiations. The primary factor is TID dose. However, the inter-strip resistance is also related to the bulk leakage current, that changes with fluence, temperature, and annealing. The values of inter-strip resistance above 100 MΩ for 2×10^{15} n_{eq}/cm^2 for proton-irradiated samples have proven that the strip isolation is sufficient for HL-LHC fluences. The most suitable PTP structure is the novel PTP structure with an extended electrode of the bias ring over the PTP gap. This full gate structure implemented in the ATLAS12 main sensor, shows a steep current increase above the low onset voltage and low effective resistance at large voltages even at the fluence of 2×10^{15} n_{eq}/cm^2. Compared to a standard structure without a gate, the new structure doubles the allowable current flowing into bias rail without increasing the onset voltage. Results from the evaluation of various sensor properties are summarized in Table 1.

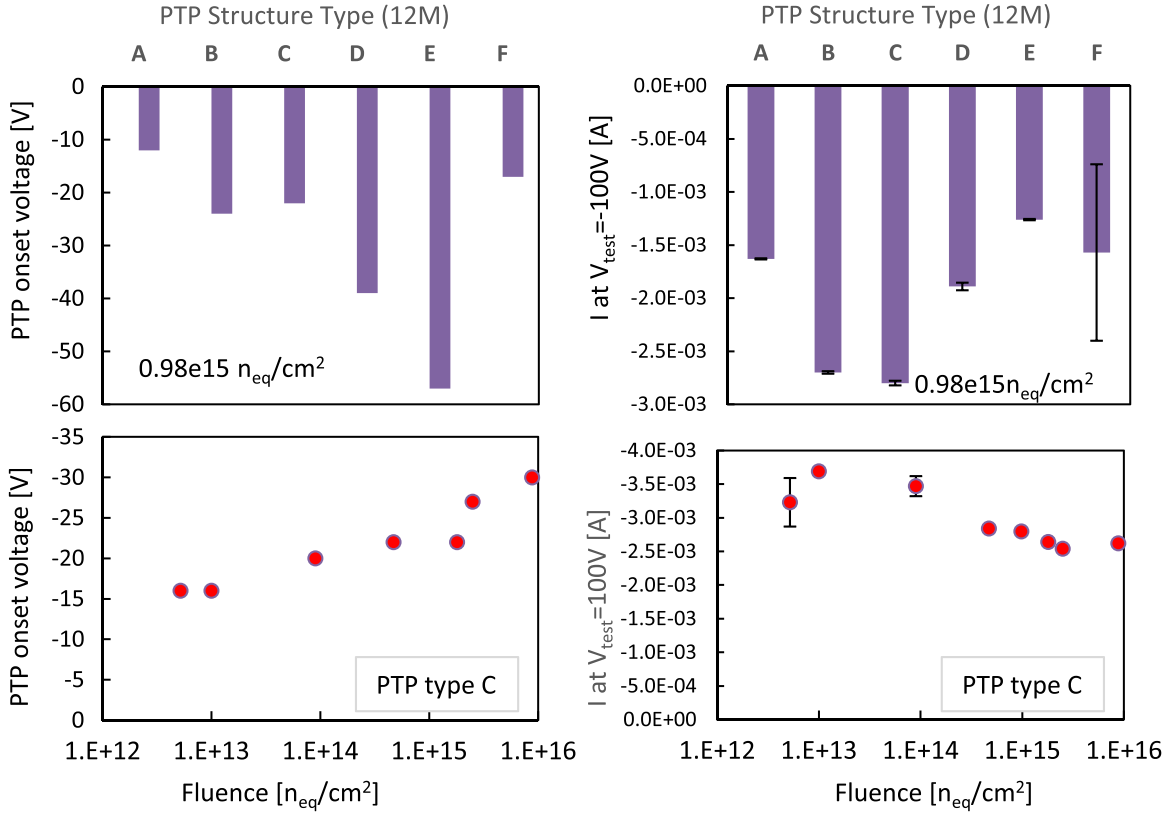

Fig. 14. PTP onset voltage (upper left) and test current at 100 V (upper right) for different types of PTP structures in sensors irradiated to 1×10^{15} n_{eq}/cm^2. Fluence dependence of V_{PTP} (bottom left) and I_{test} (bottom right) of PTP structure C.

Table 1
Summarized measurement values for various sensor properties.

	Pre-radiation	Protons 1×10^{15} [n_{eq}/cm^2]	Protons 2×10^{15} [n_{eq}/cm^2]	Gamma 100 kGy
Leakage current [$\mu A/cm^2$] (at V_{bias}=600 V)	< 0.0048 (+20 °C)	51 (−10 °C)	103 (−10 °C)	0.22 (+20 °C)
Inter-strip capacitance [pF/cm] (at 1 MHz)	0.75-0.82	0.82	0.82	0.77
Coupling Capacitance [pF/cm] (at 1 kHz)	24	24	24	–
Inter-strip resistance [GΩ/cm] (at V_{bias}=400 V)	15–65 (+20 °C)	0.5–2.2 (−20 °C)	0.3-0.7 (−20 °C)	0.0086 (+20 °C) 0.6–1.1 (−20 °C)
Bias resistance [MΩ]	1.5 ± 0.1 (+23 °C) 1.7-1.8 (−10, −20 °C)	2.0 (−20 °C)	2.1 (−20 °C)	1.7 (+23 °C)

The present surface studies have demonstrated that developed n^+-in-p strip sensors of the latest sensor design ATLAS12 show appropriate performance for operation in ATLAS Upgrade ITk.

Acknowledgments

The irradiations were performed: with protons at the University of Birmingham MC40 cyclotron, supported by the H2020 project AIDA-2020, GA number 654168, and the UK's Science and Technology Facilities Council, at Cyclotron and Radioisotope Center (CYRIC), Tohoku 45 University, with Y. Sakemi, M. Ito, and T.Wakui, at the Karlsruhe Institute of Technology (KIT) by A.Dierlamm, supported by the Initiative and Networking Fund of the Helmholtz Association, contract HA-101 (Physics at the Terascale) and the European Commission under the FP7 Research Infrastructures project AIDA, Grant agreement no. 262025, and at the LANSCE facility, Los Alamos National Laboratory; with neutrons at JSI TRIGA reactor in Ljubljana supported by the H2020 project AIDA-2020, GA no. 654168; and with γ's at Brookhaven National Laboratory (BNL) and at Institute of Nuclear Fuels (UJP), Prague.

The research was supported and financed in part by the Ministry of Education, Youth and Sports of the Czech Republic (Grant no. LG13009), the German Federal Ministry of Education and Research, and the Helmholtz Association, the European Social Fund and by the Ministry of Science, Research and Arts, Baden-Wuerttemberg, Germany, the Japan Society for Promoting Science KAKENHI-A Grant number 20244038 and KAKENHI-C Grant number 20540291, the Ministry of Education, Culture, Sports, Science and Technology-Japan, KAKENHI for Research on Priority Area Grant number 20025007 and for Scientific Research on Innovative Areas Grant number 23104002, the Slovenian Research Agency, the Spanish Ministry of Economy and Competitiveness through the Particle Physics National Program (ref. FPA2012-39055-C02-01 and FPA2012-39055-C02-02) and co-financed with FEDER funds, the financial support of the State Secretariat for Education, Research, and Innovation, the Swiss National Science Foundation and the Canton of Geneva, Switzerland, the UK Science and Technology Facilities Council (under Grant ST/M006409/1), and the United States Department of Energy, grant DE-FG02-13ER41983.

References

[1] S. McMahon, Presented at this symposium, 2015.
[2] I.-M. Gregor, Presented at this symposium, 2015.
[3] ATLAS Collaboration, Letter of Intent Phase II Upgrade, CERN-LHCC-2012-022 LHCC-I-023.
[4] I. Dawson, P. Miyagawa, ATL-GEN-2014-003, 2014.
[5] G. Casse, et al., Nucl. Instrum. Methods A487 (2002) 465–470.
[6] G. Casse, et al., IEEE Trans. Nucl. Sci. 47 (3) (2000) 527.
[7] Y. Unno, et al., Nucl. Instrum. Methods A636 (2011) S24.
[8] Y. Unno, et al., Nucl. Instrum. Methods A765 (2014) 80.
[9] Hamamatsu Photonics K.K. ⟨http://www.hamamatsu.com⟩.
[10] S. Lindgren, et al., Nucl. Instrum. Methods A636 (2011) S111.
[11] K. Hara et al., Presented at this symposium, 2015.
[12] R. Mori et al., Presented at this symposium, 2015.
[13] Karlsruhe Institute of Technology, Irradiation center, Hermann-von-Helmholtz-Platz 1, 76344 Eggenstein-Leopoldshafen, Germany, ⟨http://www.ekp.kit.edu/english/264.php⟩.
[14] P. Dervan, et al., The Birmingham Irradiation Facility, Nucl. Instrum. Methods A730 (2013) 101.
[15] L. Snoj, et al., Appl. Radiat. Isot. 70 (2012) 483–488.
[16] Solid State Gamma-ray irradiation facility, Brookhaven National Laboratory, Instr. Division, 20 N. Technology Street, Upton, NY 11973, ⟨http://www.inst.bnl.gov/facilities/ssif/⟩.
[17] Institute of Nuclear Fuels, UJP Praha, ⟨http://www.ujp.cz/⟩.
[18] ATLAS ITk Strip Sensor Collaboration, private communication.
[19] M. Moll, Nucl. Instrum. Methods A426 (1999) 87–93.
[20] M. Mikestikova et al., PoS(Vertex2014)050.
[21] S. Terada, et al., Nucl. Instrum. Methods A383 (1996) 159.
[22] K. Hara, et al., Nucl. Instrum. Methods A699 (2013) 107.
[23] J. Bohm, et al., Nucl. Instrum. Methods A636 (2011) S104.
[24] B. Hommels et al., Presented at this symposium, 2015.
[25] J. Kaplon, M. Noy, IEEE Trans. Nucl. Sci. 59 (4) (2012).
[26] www.nist.gov
[27] A. Vasilescu, G. Lindstroem, Displacement damage in silicon, on-line compilation, ⟨http://rd50.web.cern.ch/RD50/NIEL/default.html⟩, 2000.
[28] I. Mandic, et al., IEEE Trans. Nucl. Sci. 51 (4) (2004).
[29] I. Mandic, et al., Nucl. Instrum. Methods A629 (2011) 101.
[30] A. Chilingarov, et al., Nucl. Instrum. Methods A560 (2006) 118.
[31] K. Hara, Y. Ikegami, Nucl. Instrum. Methods A731 (2013) 242.
[32] K. Hara, et al., Phys. Procedia 37 (2012) 838.